Metal-organic frameworks with a sulfur-rich heterocycle: synthesis, gas adsorption properties, and metal exchange

Vadim A. Dubskikh, Anna A. Lysova, Konstantin A. Kovalenko, Denis G. Samsonenko, Danil N. Dybtsev* and Vladimir P. Fedin

Nikolaev Institute of Inorganic Chemistry, Siberian Branch of Russian Academy of Sciences, 3 Acad. Lavrentiev Ave., Novosibirsk 630090, Russia

*Author to whom correspondence should be addressed.

Materials and Methods

Instruments and Methods. The reagents and solvents (zinc nitrate hexahydrate ("Reactiv"), copper(II) nitrate hexahydrate ("Reactiv"), 1,4-diazabicyclo[2.2.2]octane (dabco) (TCI), N,N-dimethylacetamide (DMA) ("Vekton")) were at least of reagent grade and used as purchased without additional purification. Thieno[3,2-b]thiophene-2,5-dicarboxylic acid was synthesized according to the known methodology [1]. Infrared spectra of solid samples as KBr pellets were recorded using an IR-Fourier spectrometer Scimitar FTS 2000 (4000–400 cm^{-1}). The effective spectral resolution was 1 cm^{-1}. The elemental analyses were obtained using analyzers «Vario Micro-Cube» or «Euro EA 3000». The thermogravimetric analyses were carried out in Ar or He atmosphere using a NETZSCH TG 209 F1 thermoanalyzer with a heating rate of 10 $deg \cdot min^{-1}$ in the temperature range from 298 K to 873 K. The powder X-ray diffraction data were obtained on a «Shimadzu XRD 7000S» powder diffractometer (Cu-Kα irradiation, λ = 1.54178 Å) in the 2θ range from 5° to 30°. The energy-dispersive X-ray spectroscopy data were collected using a JEOL–JSM 6700F microscope combined with an EX2300BU analyzer. The porous structure was analyzed using the nitrogen adsorption technique on Quantachrome's Autosorb iQ gas sorption analyzer at 77 K. The preliminary activation of **1-Cu** was done in the following way. The required amount of the MOF was immersed in 5 mL of acetone for 5 days. Each day the supernatant was decanted, and a new portion of acetone was added to the crystals. Then, the crystals were separated by decantation of the supernatant and dried under vacuum. The next step of activation was performed in a dynamic vacuum at 453 K for 6 h directly in the gas sorption analyzer. The nitrogen adsorption–desorption isotherms were measured within the range of relative pressures from 10^{-6} to 0.995. The specific surface area was calculated from the data obtained using the conventional BET, Langmuir and DFT models. Gas (CO_2, CH_4, N_2, C_2H_2, C_2H_4 and C_2H_6) adsorption isotherm measurements at 273 and 298 K were carried out volumetrically on Quantachrome's Autosorb iQ equipped with a thermostat TERMEX Cryo-VT-12 to adjust the temperature with 0.1 K accuracy. The adsorption–desorption isotherms were measured within the range of pressures from 1 to 800

torr. The database of the National Institute of Standards and Technology [2] was used as a source of *p–V–T* relations at experimental pressures and temperatures.

X-ray Crystallography. Diffraction data for a single crystal of **1-Zn** were collected on the 'Belok/XSA' beamline (λ = 0.74500 Å, φ-scans with a step of 1.0) of the National Research Center 'Kurchatov Institute' (Moscow, Russian Federation) using a Rayonix SX165 CCD detector [3, 4]. The data were indexed, integrated and scaled, and an absorption correction was applied using the XDS program package [5]. Diffraction data for a single crystal of **1-ZnCu** were collected on an automated Agilent Xcalibur diffractometer equipped with an area AtlasS2 CCD detector (graphite monochromator, λ(MoKα) = 0.71073 Å, ω-scans with a step of 0.25°). Integration, absorption correction, and determination of unit cell parameters were performed using the CrysAlisPro program package [6]. The structures were solved by the dual space algorithm (SHELXT [7]) and refined by the full-matrix least-squares technique (SHELXL [8]) in the anisotropic approximation (except hydrogen atoms). Positions of hydrogen atoms of organic ligands were calculated geometrically and refined in the riding model. The crystallographic data and details of the structure refinements are summarized in Table S1. The structures contain a large void volume occupied with highly disordered DMA and H_2O guest molecules, which could not be refined as a set of discrete atomic positions. The final compositions of compounds were defined according to the PLATON/SQUEEZE procedure [9] (114 e^- in 977 $Å^3$ for **1-Zn** and 174 e^- in 997 $Å^3$ for **1-ZnCu**) and the data from the element (C, H, N) analysis.

Table S1. Crystal data and structure refinement for **1-Zn** and **1-ZnCu**.

Parameter	**1-Zn**	**1-ZnCu**
Empirical formula	$C_{30}H_{38}N_4O_{12}S_4Zn_2$	$C_{34}H_{49}N_5O_{14}S_4ZnCu$
M, g/mol	905.62	1008.93
T, K	100(2)	290(2)
Crystal system	*Tetragonal*	*Tetragonal*
Space group	*P*4/*mmm*	*P*4/*mmm*
a, Å	12.588(4)	12.5936(7)
c, Å	9.604(3)	9.6955(14)
V, Å^3	1521.8(11)	1537.7(3)
Z	1	1
D(calc.), g/cm^3	0.988	1.090
μ, mm^{-1}	1.094	0.920
F(000)	466	523
Crystal size, mm	0.10 × 0.10 × 0.05	0.17 × 0.17 × 0.13
θ range for data collection, deg.	3.27–31.00	2.29–29.04
Index range	$-17 \le h \le 17$, $-17 \le k \le 9$, $-13 \le l \le 10$	$-12 \le h \le 13$, $-16 \le k \le 11$, $-6 \le l \le 12$
Reflections collected / independent	7785 / 1244	4079/1099
R_{int}	0.0352	0.0465
Reflections with c $I > 2\sigma(I)$	1153	871
Goodness-of-fit on F^2	1.140	0.974
Final R indices [$I > 2\sigma(I)$]	$R_1 = 0.0489$, $wR_2 = 0.1360$	$R_1 = 0.0462$, $wR_2 = 0.1133$
R indices (all data)	$R_1 = 0.0513$, $wR_2 = 0.1373$	$R_1 = 0.0579$, $wR_2 = 0.1172$
Largest diff. peak / hole, *e*/Å^3	0.648 / − 0.811	1.827 / − 0.370

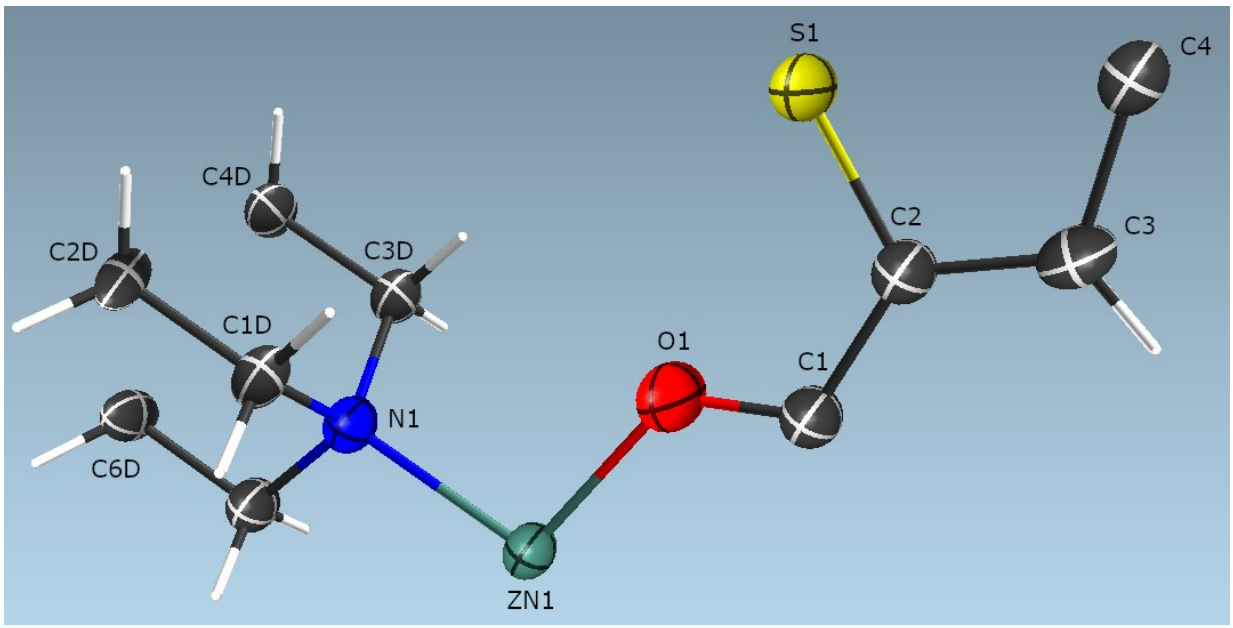

(a)

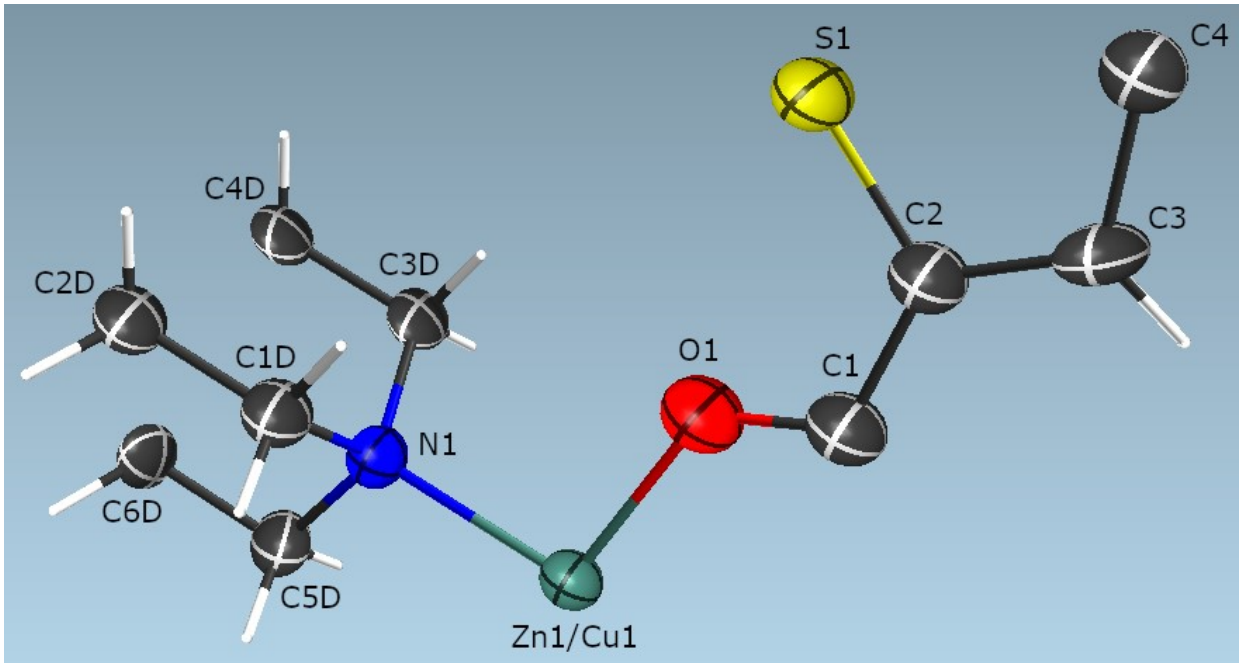

(b)

Figure S1. Asymmetric units of the structures **1-Zn** (a) and **1-ZnCu** (b). Ellipsoids are of 50% probability.

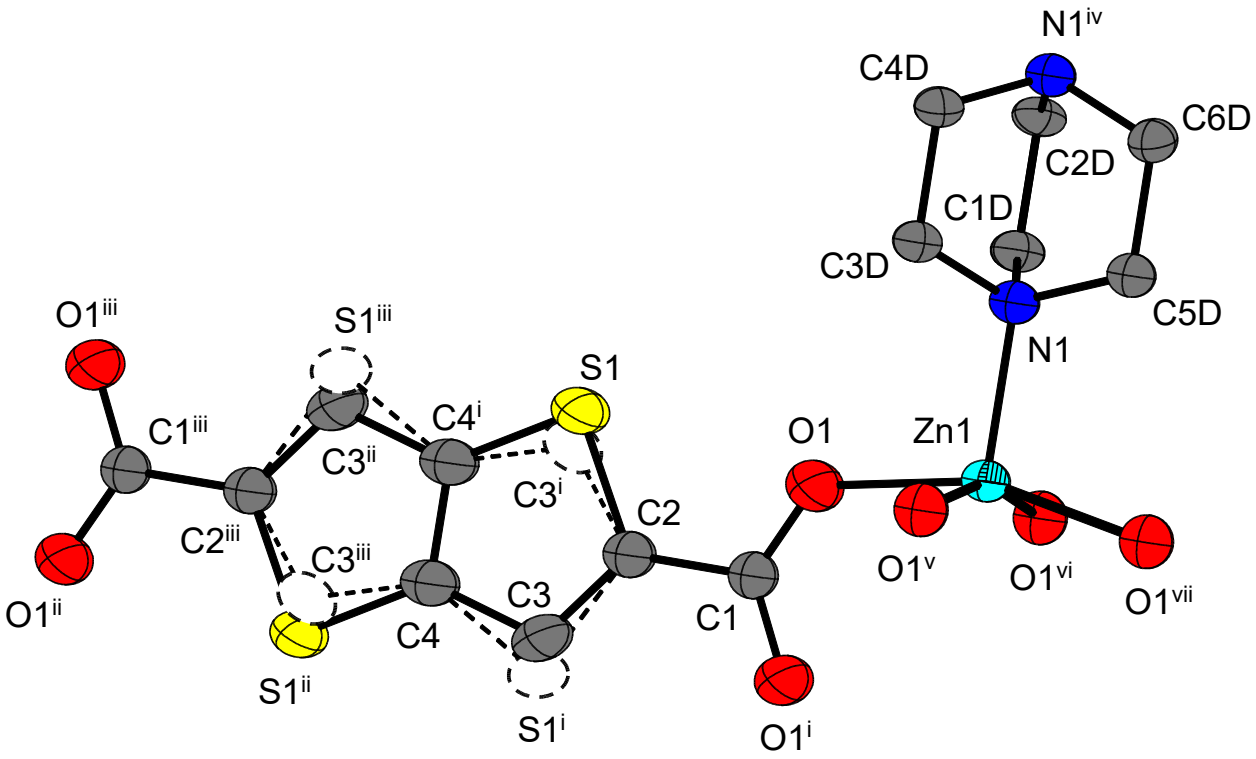

Figure S2. Coordination environment of Zn atom in the structure **1-Zn** (ellipsoids are of 50% probability; H atoms are omitted). Alternative positions of disordering S and C atoms of $ttdc^{2-}$ ligand are shown with dashed lines. Alternative positions of C atoms of dabco ligand are omitted. Symmetry codes for the related atoms: i) x, $1-y$, $1-z$, ii) $-x$, y, $1-z$, iii) $-x$, $1-y$, z, iv) x, $1-y$, $2-z$, v) $1-y$, x, z, vi) y, $1-x$, z, vii) $1-x$, $1-y$, z.

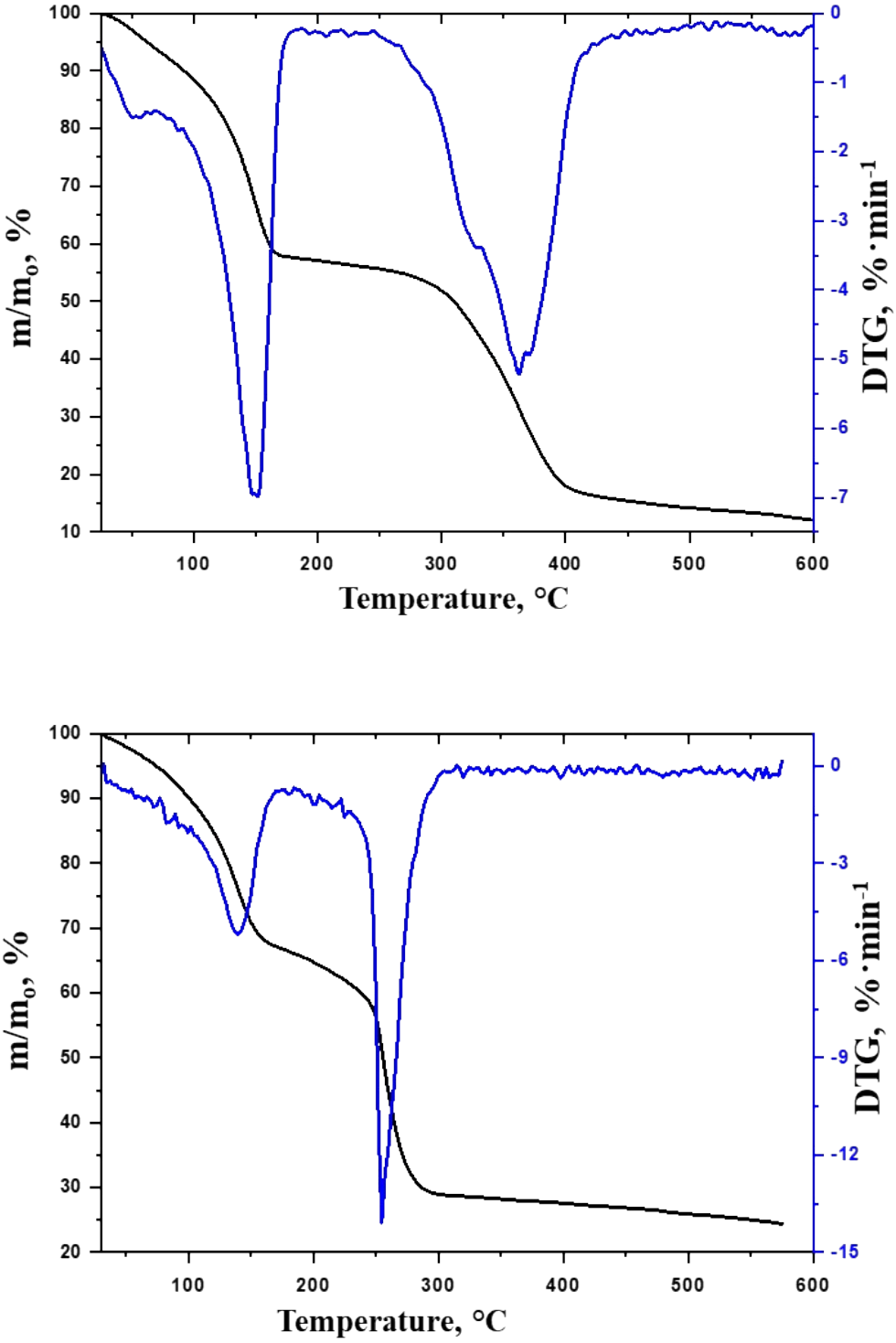

Figure S3. Thermogravimetric analysis data for **1-Zn** (top) and **1-Cu** (bottom).

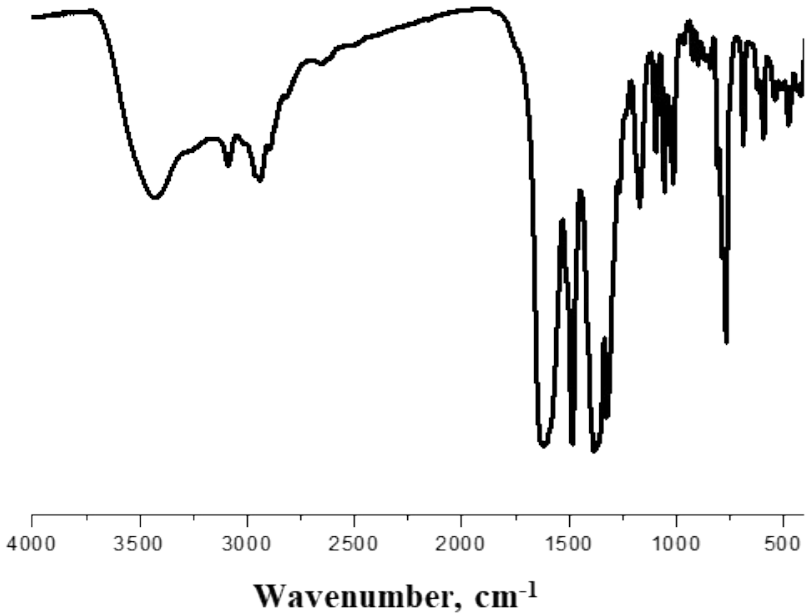

Figure S4. IR spectrum of **1-Zn**.

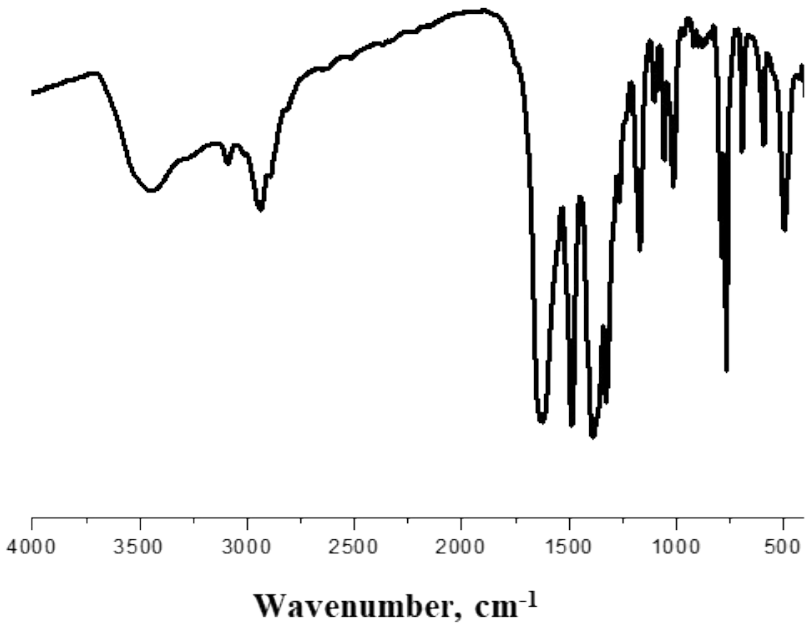

Figure S5. IR spectrum of **1-Cu**.

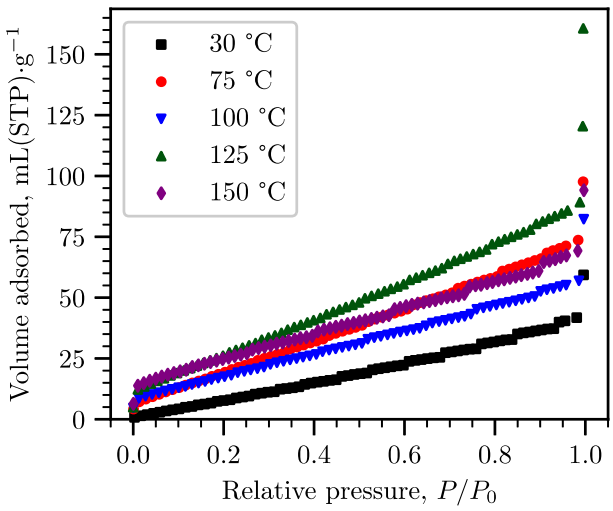

(a)

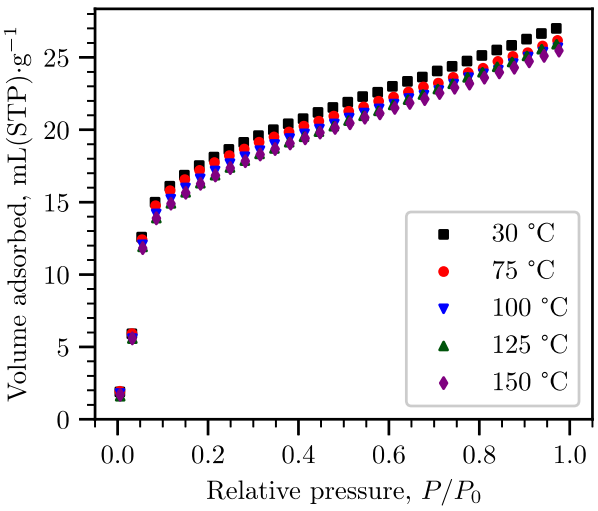

(b)

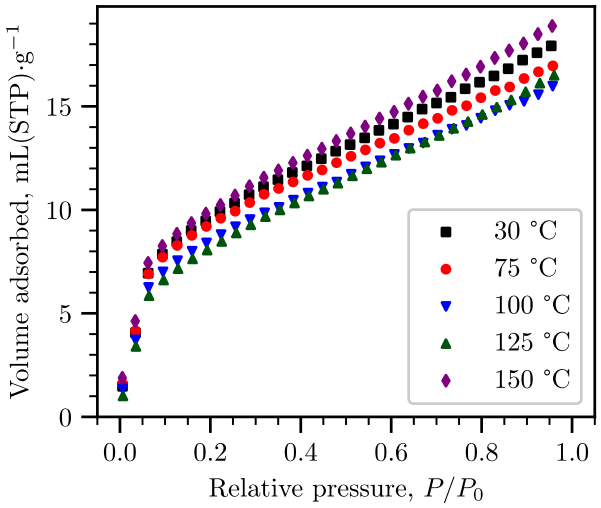

(c)

Figure S6. Adsorption isotherms for **1-Zn** activated at different temperatures during 6 h: N_2, 77 K (a) and CO_2, 195 K (b, c). Desorption curves are not shown because of the negligible adsorption-desorption hysteresis.

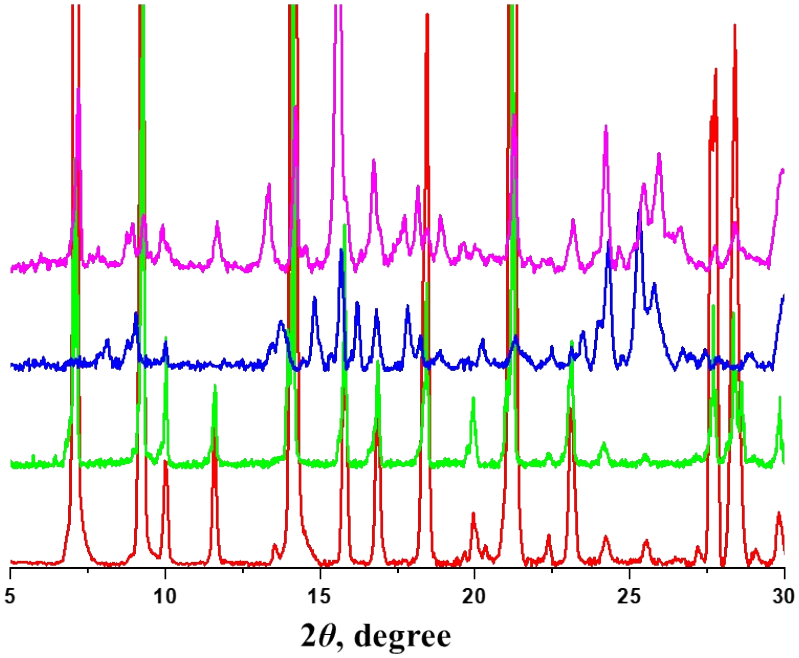

Figure S7. PXRD patterns of **1-Zn**: as-synthesized (red), activated (green), after adsorption (blue) and reactivated in DMA (pink).

Table S2. The textural parameters of the porous structure of **1-Cu**.

Specific surface area / $m^2 \cdot g^{-1}$			V_{pore} / $cm^3 \cdot g^{-1}$		$V_{ads}(N_2)^a$ / $cm^3(STP) \cdot g^{-1}$
Langmuir	**BET**	**DFT**	**Total**[a]	**DFT**	
1868	1725	1424	0.790	0.709	511

[a] measured at $P/P_0 = 0.95$.

Isotherms fit by virial equation

Gas adsorption isotherms at 273 K and 298 K were fitted by virial equation (S1) in order to calculate Henry constants and isosteric heats of adsorption.

$$lnp = lnn + \frac{1}{T}\sum_i A_i \cdot n^i + \sum_j B_j \cdot n^j \quad \text{(S1)}$$

Virial coefficients are summarized in Table S3, whereas fit plots are shown in Figure S8.

Table S3. Virial coefficients A_i and B_i for gas adsorption isotherms at 273 K and 298 K on **1-Cu**.

Gas	**Coefficients**	R^2
C_2H_6	$A_0 = -3029 \pm 31$, $A_1 = 729 \pm 36$, $A_2 = -536 \pm 26$, $A_3 = 258 \pm 18$, $A_4 = -79 \pm 7$, $A_5 = 13.8 \pm 1.4$, $A_6 = -1.25 \pm 0.14$, $A_7 = 0.046 \pm 0.006$, $B_0 = 8.30 \pm 0.11$, $B_1 = -1.01 \pm 0.11$, $B_2 = 0.225 \pm 0.025$	0.99990
C_2H_4	$A_0 = -2956 \pm 24$, $A_1 = 863 \pm 38$, $A_2 = -487 \pm 17$, $A_3 = 167 \pm 10$, $A_4 = -42 \pm 3$, $A_5 = 5.3 \pm 0.5$, $A_6 = -0.27 \pm 0.03$, $B_0 = 8.47 \pm 0.08$, $B_1 = -1.65 \pm 0.13$, $B_2 = 0.45 \pm 0.04$	0.99994
C_2H_2	$A_0 = -3636 \pm 56$, $A_1 = 1545 \pm 87$, $A_2 = -549 \pm 33$, $A_3 = 74 \pm 4$, $A_4 = -9.8 \pm 0.7$, $A_5 = 0.49 \pm 0.04$, $B_0 = 10.76 \pm 0.19$, $B_1 = -4.1 \pm 0.3$, $B_2 = 1.04 \pm 0.09$	0.99969
CO_2	$A_0 = -2602 \pm 40$, $A_1 = 1207 \pm 94$, $A_2 = -427 \pm 48$, $A_3 = 9.0 \pm 1.1$, $B_0 = 8.21 \pm 0.14$, $B_1 = -4.0 \pm 0.3$, $B_2 = 1.35 \pm 0.16$	0.99979
CH_4	$A_0 = -1886 \pm 18$, $A_1 = 27 \pm 3$, $B_0 = 7.06 \pm 0.06$	0.99964
N_2	$A_0 = -2037 \pm 70$, $B_0 = 8.71 \pm 0.25$	0.99305

C_2H_6 C_2H_4

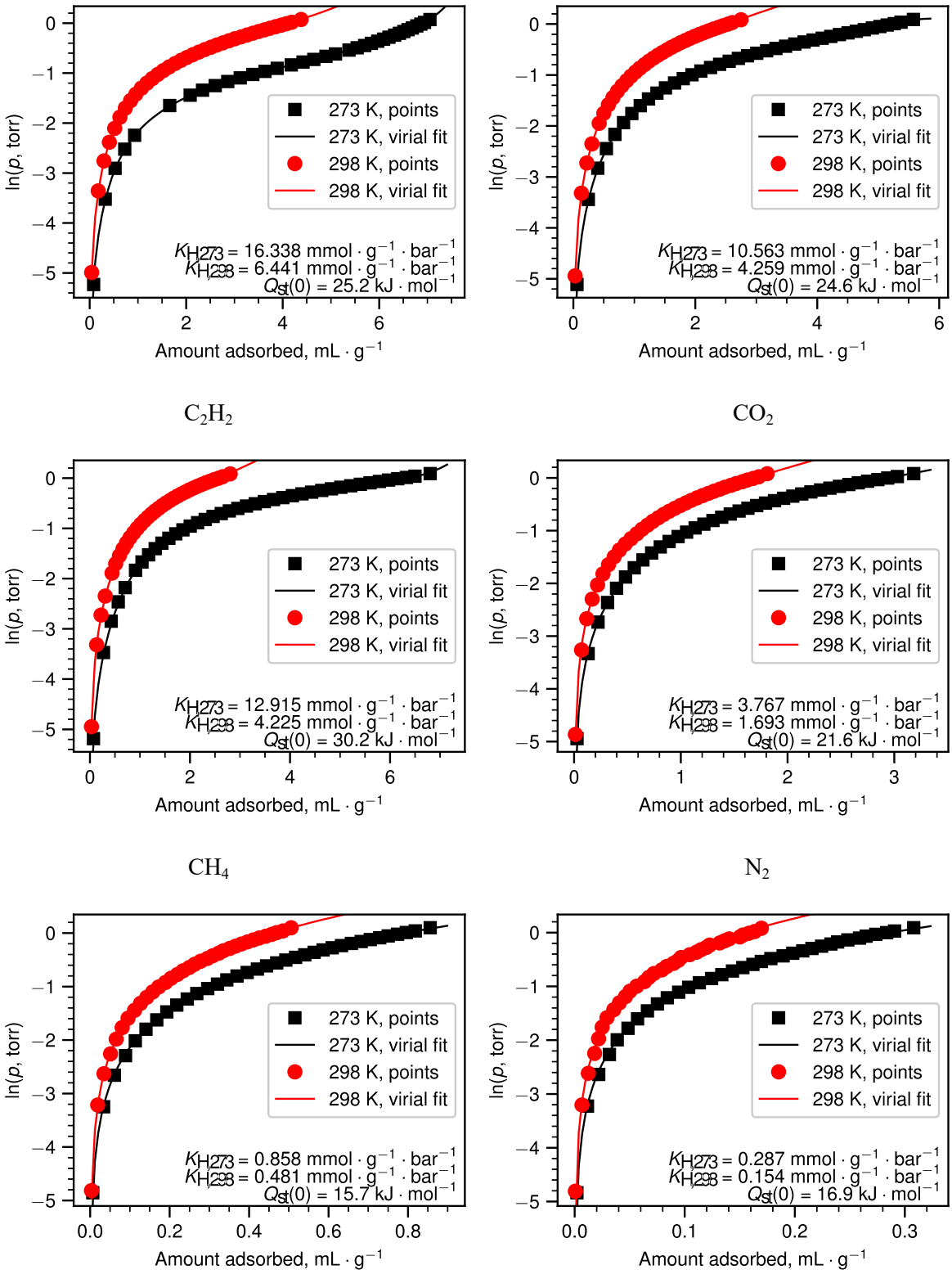

Figure S8. Fits of isotherms by virial equations.

Henry constants

Henry constants were calculated using virial coefficients by equation (S2) and summarized in Table S4:

$$K_h = exp\left[\frac{-A_0}{T} - B_0\right] \quad \text{(S2)}$$

Table S4. Henry constants for gas adsorption on **1-Cu** in mmol·g^{-1}·bar^{-1} at 273 K and 298 K.

Gas\Temperature	273 K	298 K
C_2H_6	16.338	6.441
C_2H_4	10.563	4.259
C_2H_2	12.915	4.225
CO_2	3.767	1.693
CH_4	0.858	0.481
N_2	0.287	0.154

Heats of adsorption

Isosteric heats of adsorption were calculated using virial coefficients by equation (S8) and summarized in Table 1 and Figure S9:

$$Q_{st} = -R \cdot \sum_i A_i \cdot n^i \quad \text{(S3)}$$

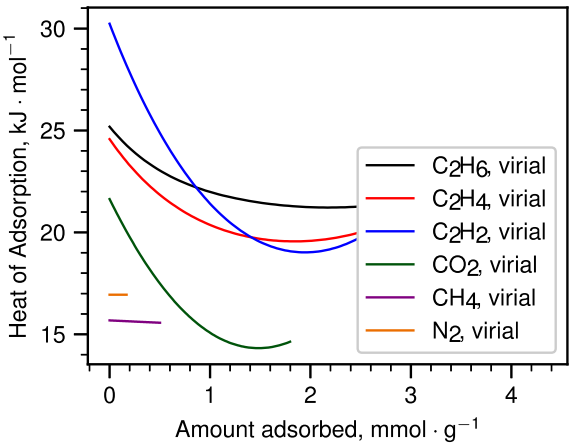

Figure S9. Isosteric heats of gases adsorption on **1-Cu**.

Fit of adsorption isotherms

For IAST calculations it is better when adsorption isotherms are fitted by the most appropriate analytical equation. We could find good fits only for CH_4 and N_2 isotherms. For fitting pressures were taken in torr, adsorption amounts were taken in $mL \cdot g^{-1}$, therefore summarized fitted parameters are in the corresponding units in Table S5. Comparison of the experimental and fitted isotherms are given in Figure S10. Adsorption isotherms of C_2 hydrocarbons and CO_2 have a complicated profile and could not be adequately fitted by the most common models, therefore, for IAST calculations we used numerical integration of these adsorption isotherms.

Equations used:

Henry: $n = k \cdot p$, Langmuir: $n = w\frac{b \cdot p}{1 + b \cdot p}$.

Fitted parameters are summarized in Table S5.

Table S5. Fitted parameters for adsorption isotherms at 273 K and 298 K.

Gas	**273 K**	**298 K**
CH_4	Langmuir $w = 199 \pm 5$, $b = 0.000129 \pm 0.000003$ $R^2 = 0.99997$	Langmuir $w = 318 \pm 41$, $b = 0.000045 \pm 0.000006$ $R^2 = 0.99989$
N_2	Henry $k = 0.008559 \pm 0.000019$ $R^2 = 0.99933$	Henry $k = 0.004726 \pm 0.000015$ $R^2 = 0.99873$

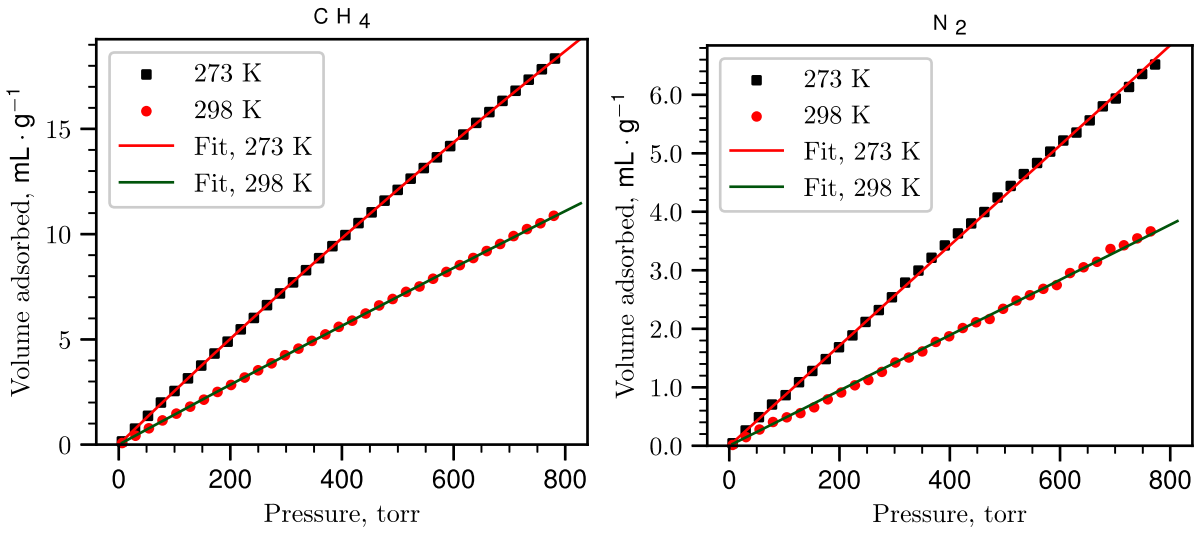

Figure S10. Fits of isotherms by appropriate models.

Selectivity calculations

Selectivity factors were evaluated by three commonly used methods:

(i) As the molar ratio of the adsorption quantities at the relevant partial pressures of the gases:

$$S = \frac{n_1/n_2}{p_1/p_2,} \tag{S4}$$

where S is the selectivity factor, n_i represents the adsorbed amount of component i, and p_i represents the partial pressure of component i.

(ii) As a ratio of Henry constants which corresponds to the slope of the adsorption isotherm at very low partial pressures:

$$S = \frac{K_{H1}}{K_{H2}} \tag{S5}$$

(iii) By ideal adsorbed solution theory (IAST). The relationship between P, y_i and x_i (P — the total pressure of the gas phase, y_i — mole fraction of the i-component in gas phase, x_i — mole fraction of the i-component in absorbed state) is defined according to the IAST theory [10]:

$$\int_{p=0}^{p=\frac{Py_1}{x_1}} n_1(p)dlnp = \int_{p=0}^{p=\frac{Py_2}{x_2}} n_2(p)dlnp \quad \text{(S6)}$$

In this case the selectivity factors were determined as:

$$S = \frac{y_2 x_2}{y_1 x_1} = \frac{x_1(1-y_1)}{y_1(1-x_1)} \quad \text{(S7)}$$

The corresponding data and graphs are shown in Table 2 and Figure S11.

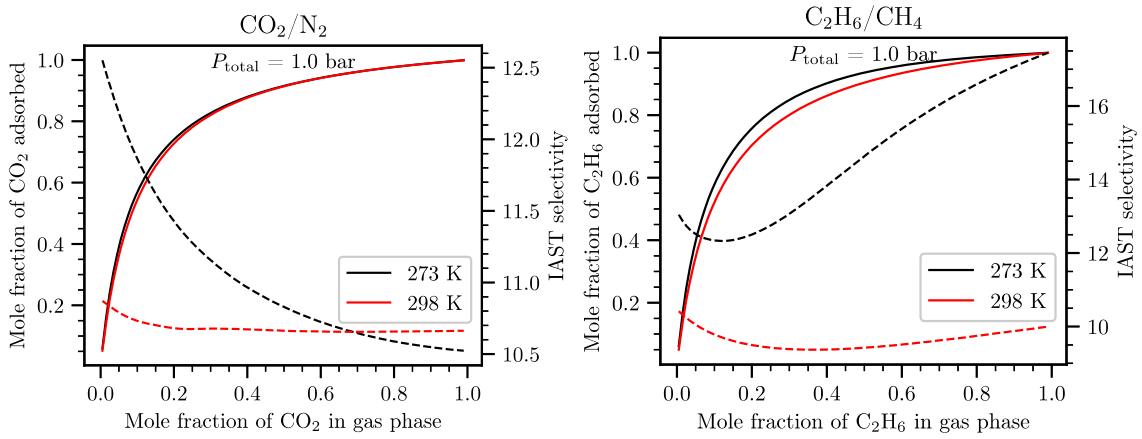

(a) (b)

Figure S11. Prediction of adsorption equilibrium by IAST (solid lines) and dependence of selectivity factors on gas phase composition (dashed lines) for binary gas mixtures: a) CO_2/N_2; b) C_2H_6/CH_4.

References:

1. Samsonova, A.M.; Bolotov, V.A.; Samsonenko, D.G.; Dybtsev, D.N.; Fedin, V.P. Network Coordination Polymers Based on Thieno[3,2-b]Thiophene-2,5-Dicarboxylic Acid. *J Struct Chem* ***2019****, 60*, 1468–1473.
2. Thermophysical Properties of Fluid Systems, Database of National Institute of Standards and Technology, NIST. Available online: http://webbook.nist.gov/chemistry/fluid/ (accessed on 29 October 2022).
3. Lazarenko, V.A.; Dorovatovskii, P.V.; Zubavichus, Y.V.; Burlov, A.S.; Koshchienko,

Y.V.; Vlasenko, V.G.; Khrustalev, V.N. High-Throughput Small-Molecule Crystallography at the 'Belok' Beamline of the Kurchatov Synchrotron Radiation Source: Transition Metal Complexes with Azomethine Ligands as a Case Study. *Crystals* **2017**, *7*, 325.

4. Svetogorov, R.D.; Dorovatovskii, P.V.; Lazarenko, V.A. Belok/XSA diffraction beamline for studying crystalline samples at Kurchatov Synchrotron Radiation Source. *Crystal Research and Technology* **2020**, *55,* 1900184.
5. Kabsch, W. "XDS". *Acta Crystallogr*. **2010**, *66*, 125–132.
6. CrysAlisPro Software system, version 1.171.42.89a. Rigaku Oxford Diffraction, Rigaku Corporation, Wrocław, Poland, **2023.**
7. Sheldrick, G.M. SHELXT – Integrated Space-Group and Crystal-Structure Determination. *Acta Crystallogr.* **2015**, *71*, 3–8.
8. Sheldrick, G.M. Crystal structure refinement with SHELXL. *Acta Crystallogr.* **2015**, *71*, 3–8.
9. Spek, A.L. PLATON SQUEEZE: A Tool for the Calculation of the Disordered Solvent Contribution to the Calculated Structure Factors. *Acta Crystallogr.* **2015**, *71*, 9–18.
10. A.L. Myers, J.M. Prausnitz, Thermodynamics of mixed-gas adsorption, AIChE l. 11 (1965) 121–127.